

Received:
05 November 2019

Revised:
26 March 2020

Accepted:
23 April 2020

<https://doi.org/10.1259/bjr.20190931>

Cite this article as:

Goodall AF, Broadbent DA, Dumitru RB, Buckley DL, Tan AL, Buch MH, et al. Feasibility of MRI based extracellular volume fraction and partition coefficient measurements in thigh muscle. *Br J Radiol* 2020; **93**: 20190931.

FULL PAPER

Feasibility of MRI based extracellular volume fraction and partition coefficient measurements in thigh muscle

^{1,2}ALEX F GOODALL, MSc, ¹DAVID A BROADBENT, PhD, ^{3,4}RALUCA B DUMITRU, MD, ⁵DAVID L BUCKLEY, PhD, ^{3,4}AI LYN TAN, MRCP, MD, ^{3,4,6}MAYA H BUCH, PhD, FRCP and ^{1,3}JOHN D BIGLANDS, PhD

¹Department Of Medical Physics and Engineering, Leeds Teaching Hospitals NHS Trust, Leeds, UK

²Department of Medical Imaging and Medical Physics, Sheffield Teaching Hospitals Foundation Trust, Sheffield, UK

³NIHR Leeds Biomedical Research Centre, Leeds, UK

⁴Leeds Institute of Rheumatic and Musculoskeletal Medicine, University Of Leeds, Leeds, UK

⁵Biomedical Imaging, University Of Leeds, Leeds, UK

⁶Centre for Musculoskeletal Research, School of Biological Sciences, Faculty of Biology, Medicine & Health, University of Manchester, Manchester, UK

Address correspondence to: Alex F Goodall

E-mail: alexgoodall@nhs.net

Objective: This study aimed to assess the feasibility of extracellular volume-fraction (ECV) measurement, and time to achieve contrast equilibrium (CE), in healthy muscles, and to determine whether in-flow and partial-volume errors in the femoral artery affect measurements, and if there are differences in the partition coefficient (λ) between muscles.

Methods: T1 was measured in the biceps femoris, vastus intermedius, femoral artery and aorta of 10 healthy participants. This was repeated alternately between the thigh and aorta for ≥ 25 min following a bolus of gadoterate meglumine. λ was calculated for each muscle/blood measurement. Time to CE was assessed semi-quantitatively.

Results: 8/10 participants achieved CE. Time to CE = 19 ± 2 min (mean \pm 95% confidence interval). Measured λ : biceps femoris/aorta = 0.210 ± 0.034 , vastus intermedius/

aorta = 0.165 ± 0.015 , biceps femoris/femoral artery = 0.265 ± 0.054 , vastus intermedius/femoral artery = 0.211 ± 0.026 . There were significant differences in λ between the muscles when using the same vessel ($p < 0.05$), and between λ calculated in the same muscle when using different vessels ($p < 0.05$).

Conclusion: ECV measurements in the thigh are clinically feasible. The use of the femoral artery for the blood measurement is associated with small but significant differences in λ . ECV measurements are sensitive to differences between muscles within the healthy thigh.

Advances in knowledge: This paper determines the time to contrast equilibrium in the healthy thigh and describes a method for measuring accurately ECV in skeletal muscle. This can aid in the diagnosis and understanding of inflammatory auto-immune diseases.

INTRODUCTION

Musculoskeletal extracellular volume-fraction (ECV) comprises the fluid-filled space between the cells within the tissue (the interstitium) and the blood plasma. It not only represents a conduit for solute exchange from the capillary to the lymphatic system but also affects cellular behaviour and fluid exchange within the tissue.¹

T₁ weighted imaging post-contrast is useful for identifying focal pathology but of limited use for diffuse disease, and is inherently qualitative.² T1 measurement allows a more objective assessment, but post-contrast values on their own are sensitive to several patient and method related factors so there has been widespread interest in other areas (e.g.

cardiology) in the estimation of ECV from pre- and post-contrast T1 measurements.²⁻⁶

In cardiac magnetic resonance (MR), ECV measurement of the myocardium by T1-mapping before and after gadolinium-based contrast agent (GBCA) administration is sensitive to focal and diffuse fibrosis, oedema and myocyte hypertrophy and is used to study a range of ischaemic and non-ischaemic subclinical myocardial pathologies.³⁻⁵ ECV mapping has been proven to be sensitive to both subtle and global changes in myocardial fibrosis that could be missed or obscured on late gadolinium-enhanced (LGE) imaging.^{2,6}

Recently, it has been shown that ECV measurements in skeletal muscle could be important in assessing and understanding inflammatory and fibrotic diseases which affect skeletal muscle. Banyersad et al⁷ measured ECV in the biceps, using a cardiac MR protocol, where they found a significant ($p < 0.0001$) increase in ECV in patients with amyloidosis compared to healthy volunteers across multiple organs and tissues. Similarly, Barison et al⁸ measured ECV of the pectoralis and latissimus dorsi (visible on cardiac MR) and found a greater ECV for patients with scleroderma compared to healthy volunteers ($23 \pm 6\%$ vs. $18 \pm 4\%$, $p < 0.01$). More recently, DeMarchi et al⁹ have shown that scleroderma can be detected in both cardiac and skeletal muscles using LGE, and Huber et al^{10,11} demonstrated that ECV measurements in skeletal muscle (again those visible on cardiac MR) offered high sensitivity and specificity (95 and 80% respectively – receiver operator characteristic (ROC) area under curve (AUC) of 0.94) in differentiating patients with idiopathic inflammatory myopathy (IIM) and healthy controls and similar levels (sensitivity – 95%, specificity – 89%, ROC AUC – 0.96) at differentiating between IIM and acute viral myocarditis patients.

However, these studies examined skeletal muscle visible at the edge of the field of view of a cardiac image, where errors due to B1 inhomogeneity could be significant. Furthermore, accurate ECV measurement requires T1 measurements pre-contrast and after contrast-agent equilibrium (CE) is established (*i.e.* when the exchange of contrast agent between the interstitium and the blood pool is such that the concentrations of contrast agent in the two volumes are equal). Previous measurements have assumed that the time delay necessary to achieve CE in skeletal muscle and the heart is the same. However, the lower resting perfusion rate of skeletal muscle may lengthen the time necessary for equilibrium to be established, and insufficient waiting times will cause errors in ECV. Therefore, it is important to establish whether or not the waiting times of around 15–20 min, that are routinely used to ensure CE in the heart, are adequate in the muscle, and what magnitude of errors in ECV measurements are likely if this order of waiting time is used for skeletal muscle. ECV measurements are likely to be sensitive to differences in tissue microstructure between the quadriceps and hamstrings.¹² It is important to establish the magnitude of these differences in the normal thigh so that differences in future studies in diseased populations can be better interpreted.

This study applies ECV measurement in the thigh because it provides large, axial muscle volumes for T1 measurement, is not affected by cardiac or breathing motion artefacts, and the femoral vessels provide relatively large regions for blood T1 measurement. However, the blood T1 measurements may be susceptible to partial volume effects, as their size may not be much larger than the clinically achievable image resolution. Additionally, inflow effects due to through-plane blood flow could compromise accuracy. An alternative approach to blood T1 measurement is to measure T1 in the aorta, where both partial volume and in-flow effects can be minimized, but this lengthens the duration, and adds to the difficulty, of the imaging protocol.

The aims of this study were to assess whether ECV measurements in the thigh are clinically feasible, to assess the time to CE in the thigh for healthy participants, to determine whether in-flow and partial volume errors in the femoral artery affect ECV measurements and to determine whether there are differences in ECV between individual thigh muscles.

METHODS AND MATERIALS

Selection of healthy participants

10 healthy participants (6 females, mean age: 35.0 years., range: 24–43 years) were imaged before and after GBCA administration between July 2017 and April 2018. Participants were recruited under regional ethics committee approval (17/EM/0079), gave informed written consent to participate in the prospective study and were free to withdraw at any time. Exclusion criteria were: 4 weeks estimated glomerular filtration rate $< 45 \text{ ml min}^{-1} 1.73 \text{ m}^{-2}$, asthma or chronic obstructive pulmonary disease, previous anaphylactic reaction to GBCAs, contraindications for MRI (claustrophobia, MR unsafe implants or foreign bodies, or pregnancy), history of rheumatic diseases, or spinal disease with neuropathy.

Imaging

Volunteers were imaged on a Siemens Verio 3 T scanner (Siemens Healthcare), feet-first supine with two Siemens small 4-channel flexible-coils (35 x 17 cm left-right by foot-head) placed with the inferior edge approximately 4 cm above the patella for the thigh images, and a Siemens body 18 matrix-coil placed on the chest for the aorta images. The contralateral leg was shielded using an RF blanket. Chest images were acquired at an oblique sagittal angle imaging from the top the aortic arch following the track of the aorta.

Images were acquired using an inversion recovery steady-state free precession sequence. A non-selective inversion pulse was used to minimise in-flow effects. An image acquired without an inversion pulse [inversion time (TI) = 0 ms] was used to obtain the initial estimate for the signal at equilibrium (S_0), in fitting the monoexponential recovery equation. Imaging parameters are given in Table 1.

Contrast [0.1 mmol kg^{-1} gadoterate meglumine (Dotarem, Guerbet LLC)] was administered intravenously as a single bolus and then alternate aorta and thigh post-contrast scans were then acquired sequentially for at least 25 min. As the signal from TI = 0 ms was only used as an initial guess for the S_0 in the fitting equation, and not used as a data point, it was excluded from the post-contrast scans to increase the temporal resolution of the data, but included pre-contrast to increase the speed and accuracy of the T1-fitting.

The pre-contrast TR for each sequence was set to 10 s so as to be greater than five times the maximum T1 for the expected biological range. The post-contrast TR was shortened to 6 s to reflect the reduction in T1 from the GBCA-administration and to decrease the time delay between acquisitions. TIs were also shortened post-contrast to reflect the increased rate of recovery. The mean time between the start of the two sequences was 73 s.

Table 1. Pre- and post-contrast acquisition parameters for the thigh and aorta sequences

Parameter	Pre-contrast values	Post-contrast values
TR (ms)	1000	6000
TE (ms)	1.83	1.83
TI (ms)	0, 80, 120, 160, 640, 3550, 5100	80, 120, 160, 320, 640, 2550
Flip angle (°)	60	60
Slice thickness (mm)	5	5
Bandwidth (Hz/px)	930	930
FoV – Leg (mm x mm)	250 x 250	250 x 250
FoV – Aorta (mm x mm)	300 x 300	300 x 300
Matrix size	256 x 256	256 x 256

FOV, field of view; TE, echo time; TI, inversion time; TR, repetition time.

Contrast [0.1mmol kg⁻¹ gadoterate meglumine (Dotarem, Guerbet LLC)] was administered intravenously as a single bolus.

Data analysis

Measurement of T1 in-vivo

Image analysis was performed using MATLAB (MATLAB R2015a, The MathWorks Inc. Natick, MA, 2015) and ImageJ (ImageJ 1.51k, Rasband, W.S., ImageJ, U. S. National Institutes of Health, Bethesda, MD, <https://imagej.nih.gov/ij/>, 1997–2018).

Regions of interest (ROIs) were contoured within the muscles avoiding muscle fascia. For the femoral artery, a small circular ROI was created around a user-defined centre, set within the vessel, ensuring that the ROI fell fully within the vessel to minimise partial volume effects (Figure 1a). In the aorta, a rectangular ROI was created around a central line drawn by the user. The width was chosen to avoid inclusion of the vessel wall and was long enough to span the extent of at least three vertebrae. The ROI was located towards the inferior end of the aorta to minimise in-flow effects (Figure 1b). All ROIs were drawn using ImageJ. ROIs were copied across all images manually adjusting for any movement between images.

T1 values for each ROI were obtained by fitting the mean signal within the ROIs at the different TIs to a monoexponential recovery equation: -

$$S = S_0 \cdot \left(1 - \left([1 - \cos(\theta)] \cdot e^{-\frac{TI}{T_1}} \right) \right)$$

Where θ is the inversion angle, to the mean signal intensities from each ROI at each time point using a non-linear least squares fitting algorithm (lsqcurvefit, MATLAB R2015a). S_0 , θ , and T_1 are all free parameters in the fit. Constraints were applied so that S_0 and T_1 were positive, and θ was between 0 and π radians.

The signal output of the scanner was not phase corrected from the inversion recovery, and so only the magnitude of the signal data was obtained. To fit the magnitude data to the monoexponential recovery equation the method of Messroghli et al¹³ was used. The sign of the signal from each TI point, starting with the lowest TI, was changed sequentially from positive to negative, keeping previously changed values negative, and the fitting algorithm was run for each combination. The coefficient of determination (R^2) for each fit was recorded and the fit with the maximum R^2 value was chosen. Data points with values below 10% of the maximum signal in the sequence were considered to be influenced by the Rician noise floor and were therefore excluded from the fitting.

Determining the partition coefficient and time to contrast equilibrium

For each time point the partition coefficient, λ , was calculated using: -

$$\lambda = \frac{R1_{muscle}}{R1_{blood}} \left(= \frac{[CA_{muscle}]}{[CA_{blood}]} = \frac{ECV_{muscle}}{ECV_{blood}} \right)$$

Where: -

$$R1 = \frac{1}{T_1}$$

To ensure that that blood and muscle values from the same time point were used, blood $\Delta R1$ values were temporally interpolated using a biexponential decay model to reflect the more rapid decay from the GBCA entering the extravascular space and the slower decay from renal extraction.¹⁴ This allowed a

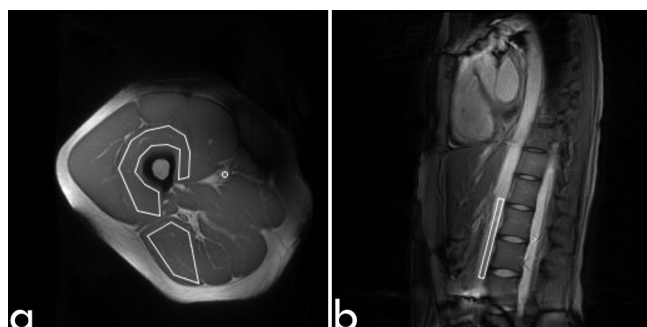


Figure 1. (a) Example ROIs on for vastus intermedius, biceps femoris, and femoral artery on the thigh images. (b) Example ROI on for aorta on the chest images. ROI, region of interest.

more physiologically appropriate interpolation of the blood $\Delta R1$ values than linear interpolation.

As GBCAs distribute themselves only within extracellular space in the interstitium and the blood–plasma within the vasculature, then at equilibrium the ratio of the GBCA concentrations will be equal to the ratio of ECV fractions (assuming sufficiently rapid water exchange) so that the effect of the contrast agent can be assumed to be averaged over the whole tissue volume. The ECV fraction in the blood is the plasma volume fraction, equal to $1 - \text{haematocrit}$ ($1 - \text{hct}$), and so the ECV fraction in the muscle can be calculated (below) if the haematocrit is known, or estimated using an assumed value (e.g. 0.42 haematocrit as found by Jacob et al.)¹⁵

$$ECV = \lambda \times (1 - \text{hct})$$

λ was then plotted against time since contrast administration and a third-order polynomial was fitted to smooth the data. Example figures of the biexponential and third-order polynomial fits are shown for one volunteer who did not reach equilibrium (Figure 2a–c) and for one who did (Figure 3a–c).

Time to CE was defined as the next acquired scan time point after the gradient of the polynomial reached zero. To investigate the magnitude of errors in ECV if the post-contrast imaging was limited to a clinically feasible time frame a pragmatic post-contrast delay time of 20 min¹⁶ was chosen.

Statistical analysis

All statistical analysis was performed in MATLAB. Comparisons between groups were performed using a Wilcoxon signed-rank test (significance at $p < 0.05$). All results are reported as mean \pm 95% confidence interval ($1.96 \times \sigma/\sqrt{n}$). No volunteers were excluded.

RESULTS

Measurement of T1 *in-vivo*

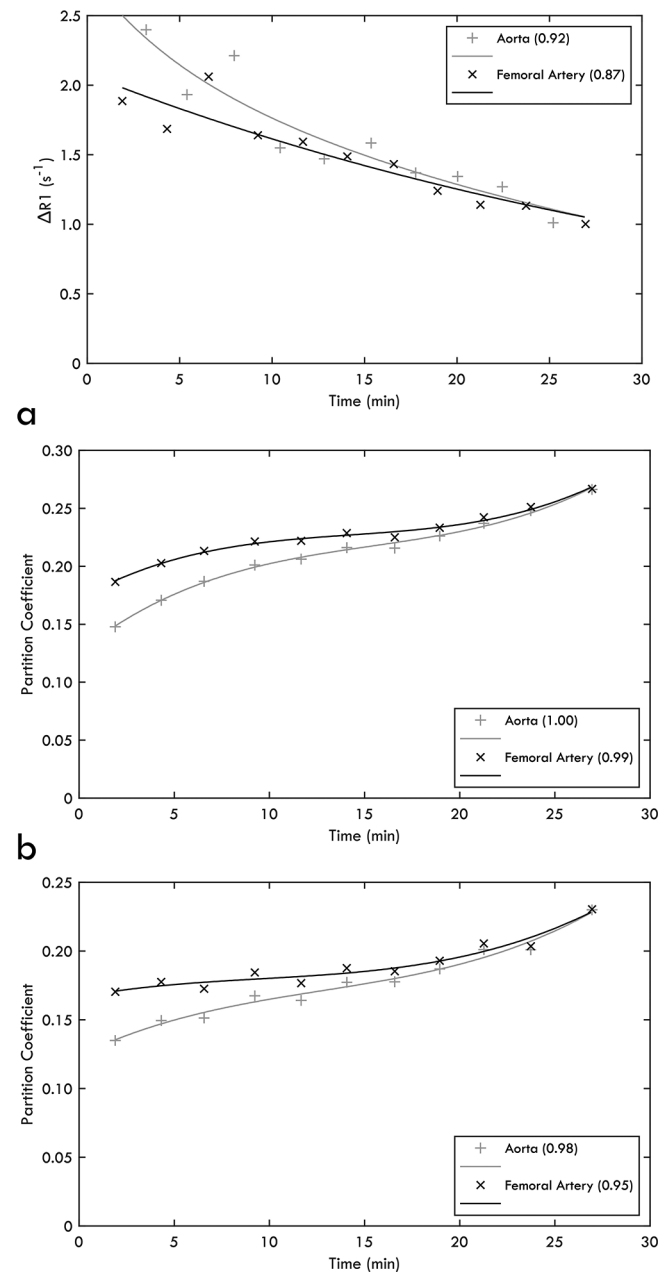
There was no significant difference between the native T1 values of blood in the aorta compared to the femoral artery (aorta 1808 ± 166 ms, femoral artery 1873 ± 298 ms; $p = 0.70$), but there was a significant difference between the T1 values of the two muscles (biceps femoris 1352 ± 21 ms, vastus intermedius 1387 ± 42 ms; $p < 0.005$) (Figure 4).

Determining the partition coefficient and time to contrast equilibrium

A CE plateau was achieved in 8/10 healthy participants. There was no significant difference between the times to CE for the two muscles ($p = 0.3$) or between measurements made using the aorta or femoral artery for the blood values ($p = 1.0$) (Table 2 and Figure 5a).

Partition coefficient (λ) measurements at equilibrium (Table 2 and Figure 5b) were significantly higher in the biceps femoris compared to the vastus intermedius, regardless of which vessel was used (aorta: $p = 0.03$, femoral artery: $p = 0.02$). λ is also higher when using the femoral artery for blood $\Delta R1$ values,

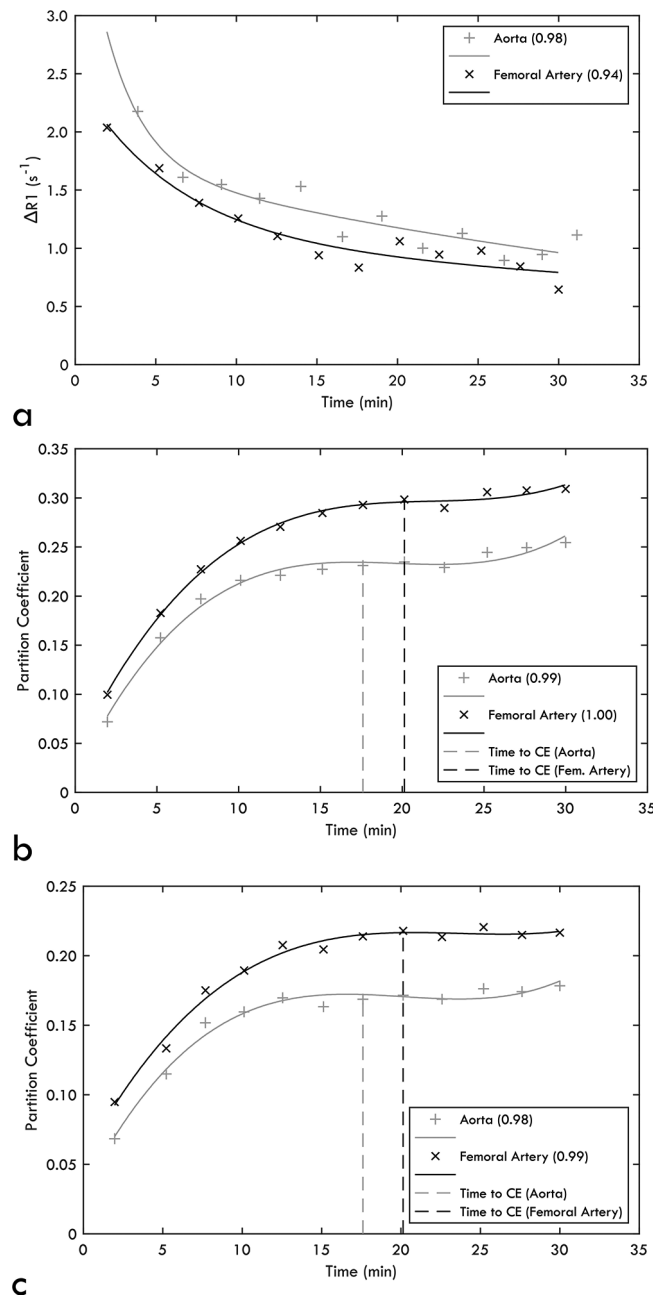
Figure 2. For a volunteer who did not reach equilibrium: (a) measured change in relaxation rate of blood measured in the aorta and femoral artery, with biexponential fits. (b) Partition coefficient in the Biceps Femoris against time graphs for aorta and femoral artery, with third-order polynomial fit. (c) Partition coefficient in the Vastus Intermedius against time graphs for aorta and femoral artery, with third-order polynomial fit. Coefficient of determination (R^2) for fit is given in brackets.



regardless of the muscle used (biceps femoris: $p = 0.01$, vastus intermedius: $p = 0.01$).

Comparisons between λ values measured using the values at 20 min (Figure 5c) and the value at equilibrium (or the end time point of the experiment for participants who didn't reach CE) are given in Table 2. Differences in λ ($\Delta\lambda$) between equilibrium and

Figure 3. For a volunteer who did reach equilibrium: (a) measured change in relaxation rate of blood measured in the aorta and femoral artery, with biexponential. (b) Partition coefficient in the Biceps Femoris against time graphs for aorta and femoral artery, with third order polynomial fit. (c) Partition coefficient in the Vastus Intermedius against time graphs for aorta and femoral artery, with third order polynomial fit. Coefficient of determination (R^2) for fit is given in brackets.

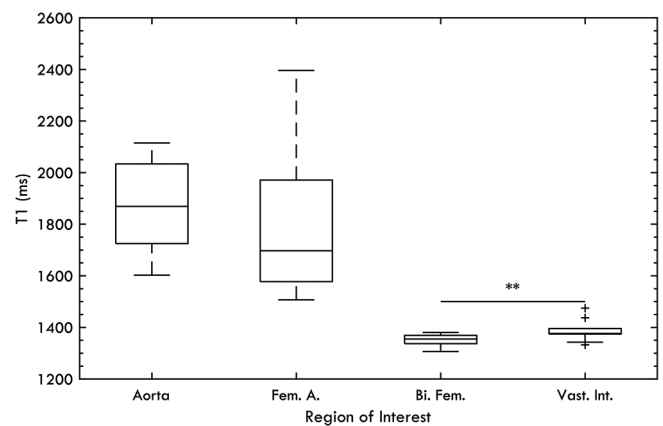


20 min (Figure 5d) were small (0.002–0.004) and not significant ($p = 0.16$ –0.94) for all muscle vessel combinations.

DISCUSSION

This study has shown that ECV measurements are feasible in thigh muscle and that they are sensitive to differences between muscles. In most cases, CE was achieved in a clinically practicable

Figure 4. Pre-contrast T1s for the four ROIs. There is a significant difference between the T1 of the biceps femoris and the vastus intermedius (** $p < 0.01$) but not the two vessels. ROI, region of interest.



time frame of 20 min. There were small but significant changes in λ between the femoral artery and aorta-based blood $\Delta R1$ measurements.

Measured pre-contrast T1 measurements were comparable to the literature.^{17–21} The observed difference in pre-contrast T1 measurements between the biceps femoris and the vastus intermedius is consistent with known differences in muscle fibre populations and fat-fractions between quadriceps and hamstrings.^{22–25} In general, T1 measurements in blood had a larger standard deviation than those in muscle, which could be due to flow effects, variability in haematocrit, or blood oxygenation levels.^{26–28}

In most cases, the time to CE was achieved in <24 min. For those cases, if a pragmatic cut-off time of 20 min had been used, the resulting error in the estimated ECV would be less than 1% (assuming 0.42 haematocrit).^{15,29} This suggests that skeletal-muscle ECV measurements would be achievable within a clinically relevant time scale with very small errors due to poor contrast equilibrium. However, 2/10 healthy participants did not reach CE within the time frame of the experiment. In these cases, the mean difference between λ measured at the end of the study and that measured after 20 min would lead to an underestimation of the ECV approximately equal to 1% for both biceps femoris and vastus intermedius across both blood measurements. Such errors are unlikely to obscure clinical differences in ECV^{7–11} (which are of the order of 5%). Therefore, we recommend a pragmatic post-contrast imaging time of 20 min. The reason for longer CE times compared to cardiac studies may be due to lower perfusion in the muscle, and so it takes longer for the relative concentrations of contrast in the blood and muscle to reach equilibrium. It may be advisable to require some exercise prior to skeletal muscle ECV measurements to ensure sufficiently high flow rates. This should be addressed in further work.

There was a significant, and systematic, difference in λ at 20 min using blood measurements taken from the aorta compared to the femoral artery, which may be due to inflow or partial volume

Table 2. Mean time to CE, and partition-coefficients measured at three different time points (at equilibrium, if reached, at approximately 20 min, and at the end of the scanning session) for all muscle vessel pairs

Muscle	Biceps femoris		Vastus Intermedius	
	Aorta	Femoral artery	Aorta	Femoral artery
Vessel				
Time to CE (min)	19.2 ± 6.1	20.4 ± 3.9	19.1 ± 4.9	18.9 ± 5.0
λ at Equilibrium	0.210 ± 0.034	0.265 ± 0.054	0.165 ± 0.015	0.211 ± 0.026
λ at 20 min	0.212 ± 0.027	0.262 ± 0.045	0.174 ± 0.016	0.213 ± 0.023
λ at End	0.225 ± 0.030	0.273 ± 0.042	0.182 ± 0.019	0.219 ± 0.021
$\Delta\lambda$: 20 min – Equilibrium ($n = 8$)	-0.002 ± 0.005	-0.002 ± 0.005	0.004 ± 0.005	0.003 ± 0.007
$\Delta\lambda$: End - 20 min ($n = 2$)	0.032	0.032	0.024	0.023

CE, contrast equilibrium.

The reported difference in partition coefficient ($\Delta\lambda$) is the difference between λ at 20 min and at equilibrium if reached, and at the end of the time-course if not.

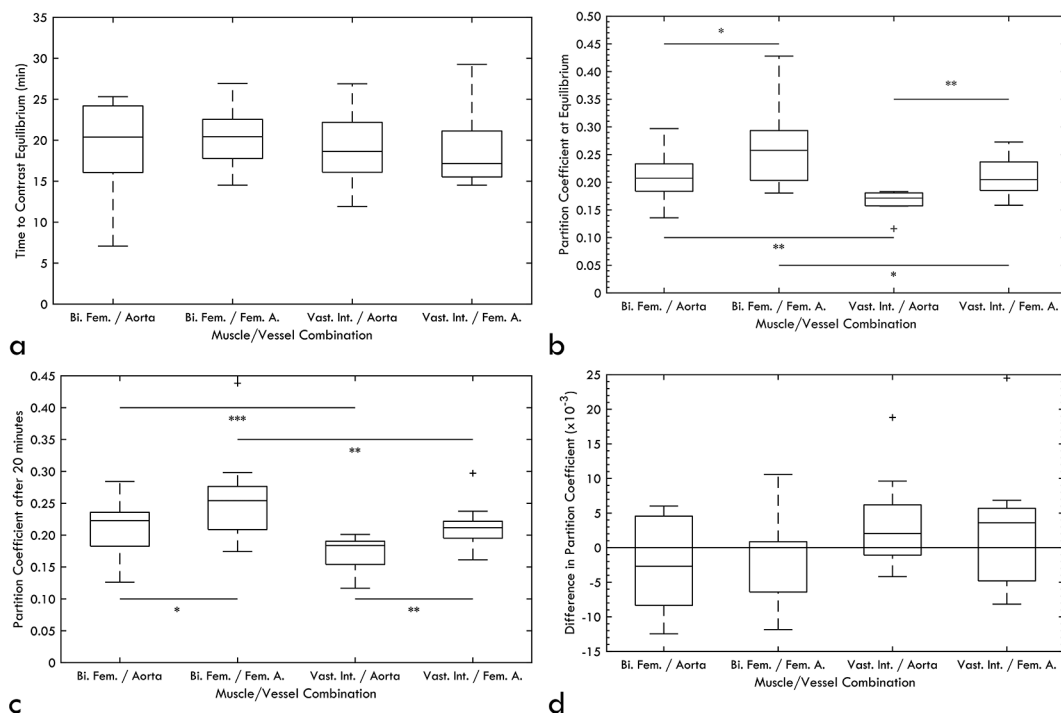
effects. The mean difference in λ between both muscles using the femoral artery compared to the aorta would cause an approximate difference in the measured ECV of $2.0 \pm 1.7\%$. This is again too small to obscure clinical differences but may justify preferring the aorta for blood measurements.

The difference in λ for the biceps femoris and vastus intermedius could be due to different proportions of type-1 and type-2 fibres between these muscles. Vincensini et al³⁰ found a higher ECV in muscles with higher type-1 fibre percentage (in rabbits) and as the hamstrings have more type-1 fibres than the quadriceps^{24,25} this could explain the greater λ in the biceps femoris

observed in this study. This is consistent with other studies^{22–25} where differences in diffusion and fat fraction have also been noted. Estimated ECVs for the two muscle populations (aorta/femoral artery: *biceps femoris* – $9 \pm 2\% / 12 \pm 4\%$; *vastus intermedius* – $7 \pm 1\% / 9 \pm 1\%$) are consistent with ECV measurements in skeletal muscle in the literature ($10 \pm 2\%$ - Huber et al^{10,11} and 9% - Banyersad et al).⁷

We acknowledge a number of limitations in this study, including small sample size. The use of magnitude images incorporates small errors in T1, and this could have been improved by using a phase-sensitive recovery sequence. Although respiratory and

Figure 5. (a) Time to contrast equilibrium for all muscle/vessel combinations. There was no significant difference in CE values between any muscle/vessel combinations. (b) Partition coefficient values for the volunteers who reached equilibrium for all muscle/vessel combinations (* $p < 0.05$, ** $p < 0.01$). (c) Partition coefficient values for all volunteers at approximately 20 min (** $p < 0.005$). (d) The difference in the measured partition coefficient at 20 min for the volunteers who reached equilibrium compared to the equilibrium value. There was no significant difference between the value at 20 min and that at equilibrium.



cardiac motion artefacts did not affect the region of the aorta where measurements were taken, gating techniques could have improved the quality of the data. A longer imaging time would have ensured that equilibrium was reached but could have reduced compliance and lead to discomfort and gross motion artefacts. The thigh images were not fat-suppressed which could have caused a biexponential T1 recovery due to the different T1 values of fat and water. To estimate the impact of fat on our ECV measurements fitting was repeated using a biexponential equation with an assumed fat T1 of 370 ms¹⁶ and a fat-fraction of 5% in the vastus intermedius and 10%³¹ in the biceps femoris. There was a small but significant difference in ECV at equilibrium (<1%, $p < 0.05$), and in the time to CE (3 min, $p < 0.05$). Errors of this magnitude would not be sufficient to alter the conclusions of this study.

CONCLUSION

ECV measurements in the thigh are clinically feasible and most healthy participants would reach CE using a post-contrast delay of 20 min. In cases where CE time is uncharacteristically long, using such a 20 min delay time would not induce ECV errors

greater than 4%. There are small errors in partition coefficient associated with using the femoral artery for blood-pool measurements, so aortic blood-pool measurements are recommended wherever possible. There are significant differences in partition coefficient between the biceps femoris and vastus intermedius, which are consistent with known differences in muscle fibre populations.

ACKNOWLEDGEMENT

We acknowledge the work of the radiographers Brian Chaka and Dominic Bertham, and of Bilkis Begum who helped cannulate and prepare volunteers for MRI. The research is supported by the National Institute for Health Research (NIHR) infrastructure at Leeds. The views expressed are those of the authors and not necessarily those of the NHS, the NIHR or the Department of Health.

CONFLICT OF INTEREST

The authors of this manuscript declare no relationships with any companies, whose products or services may be related to the subject matter of the article.

REFERENCES

- Scallan J, Huxley VH, Korthuis RJ. Capillary Fluid Exchange: Regulation, Functions, and Pathology. In: *Capillary Fluid Exchange: Regulation, Functions, and Pathology*. 2. San Rafael (CA: Morgan & Claypool Life Sciences; 2010 01. 1–94. <https://www.ncbi.nlm.nih.gov/books/NBK53446/>. doi: <https://doi.org/10.4199/C00006ED1V01Y201002I SP003>
- Schelbert EB, Messroghli DR. State of the art: clinical applications of cardiac T1 mapping. *Radiology* 2016; **278**: 658–76. doi: <https://doi.org/10.1148/radiol.2016141802>
- Kellman P, Wilson JR, Xue H, Bandettini WP, Shanbhag SM, Druey KM, et al. Extracellular volume fraction mapping in the myocardium, part 2: initial clinical experience. *J Cardiovasc Magn Reson* 2012; **14**: 64. doi: <https://doi.org/10.1186/1532-429X-14-64>
- Ugander M, Oki AJ, Hsu L-Y, Kellman P, Greiser A, Aletras AH, et al. Extracellular volume imaging by magnetic resonance imaging provides insights into overt and sub-clinical myocardial pathology. *Eur Heart J* 2012; **33**: 1268–78. doi: <https://doi.org/10.1093/eurheartj/ehr481>
- Haaf P, Garg P, Messroghli DR, Broadbent DA, Greenwood JP, Plein S. Cardiac T1 mapping and extracellular volume (ECV) in clinical practice: a comprehensive review. *J Cardiovasc Magn Reson* 2016; **18**: 89. doi: <https://doi.org/10.1186/s12968-016-0308-4>
- Perea RJ, Ortiz-Perez JT, Sole M, Cibeira MT, de Caralt TM, Prat-Gonzalez S, et al. T1 mapping: characterisation of myocardial interstitial space. *Insights Imaging* 2015; **6**: 189–202. doi: <https://doi.org/10.1007/s13244-014-0366-9>
- Banyersad SM, Bandula S, Sado D, Pinney JH, Gibbs SD, Maestrini V, et al. Multiorgan ECV as measured by EQ-MRI in systemic amyloidosis. *J Cardiovasc Magn Reson* 2013; **15**(Suppl 1): O34 doi: <https://doi.org/10.1186/1532-429X-15-S1-O34>
- Barison A, Aquaro GD, Pugliese NR, Cappelli F, Chiappino S, Vergaro G, et al. Measurement of myocardial amyloid deposition in systemic amyloidosis: insights from cardiovascular magnetic resonance imaging. *J Intern Med* 2015; **277**: 605–14. doi: <https://doi.org/10.1111/joim.12324>
- Barison A, Gargani L, De Marchi D, Aquaro GD, Guiducci S, Picano E, et al. Early myocardial and skeletal muscle interstitial remodelling in systemic sclerosis: insights from extracellular volume quantification using cardiovascular magnetic resonance. *Eur Heart J Cardiovasc Imaging* 2015; **16**: 74–80. doi: <https://doi.org/10.1093/ehjci/jeu167>
- Huber AT, Lamy J, Bravetti M, et al. Comparison of Mr T1 and T2 mapping parameters to characterize myocardial and skeletal muscle involvement in systemic idiopathic inflammatory myopathy (IIM). *Eur Radiol* 2019; 1–9.
- Huber AT, Bravetti M, Lamy J, Bacoyannis T, Roux C, de Cesare A, et al. Non-Invasive differentiation of idiopathic inflammatory myopathy with cardiac involvement from acute viral myocarditis using cardiovascular magnetic resonance imaging T1 and T2 mapping. *J Cardiovasc Magn Reson* 2018; **20**: 1–11. doi: <https://doi.org/10.1186/s12968-018-0430-6>
- Farrow M, Grainger AJ, Tan AL, Buch MH, Emery P, Ridgway JP, et al. Normal values and test-retest variability of stimulated-echo diffusion tensor imaging and fat fraction measurements in the muscle. *Br J Radiol* 2019; **92**: 20190143. doi: <https://doi.org/10.1259/bjr.20190143>
- Messroghli DR, Radjenovic A, Kozierke S, Higgins DM, Sivanathan MU, Ridgway JP. Modified Look-Locker inversion recovery (MOLLI) for high-resolution T1 mapping of the heart. *Magn Reson Med* 2004; **52**: 141–6. doi: <https://doi.org/10.1002/mrm.20110>
- Weinmann HJ, Brasch RC, Press WR, Wesbey GE, Websey GE. Characteristics of gadolinium-DTPA complex: a potential NMR contrast agent. *AJR Am J Roentgenol* 1984; **142**: 619–24. doi: <https://doi.org/10.2214/ajr.142.3.619>
- Jacob M, Annaheim S, Boutellier U, Hinske C, Rehm M, Breymann C, et al. Haematocrit is invalid for estimating red cell volume: a prospective study in male volunteers. *Blood Transfus* 2012; **10**: 471–9. doi: <https://doi.org/10.2450/2012.0111-11>

16. Messroghli DR, Moon JC, Ferreira VM, Grosse-Wortmann L, He T, Kellman P, et al. Clinical recommendations for cardiovascular magnetic resonance mapping of T1, T2, T2* and extracellular volume: a consensus statement by the Society for cardiovascular magnetic resonance (SCMR) endorsed by the European association for cardiovascular imaging (EACVI). *J Cardiovasc Magn Reson* 2017; **19**Vol. doi: <https://doi.org/10.1186/s12968-017-0389-8>
17. Gold GE, Han E, Stainsby J, Wright G, Brittain J, Beaulieu C. Musculoskeletal MRI at 3.0 T: relaxation times and image contrast. *American Journal of Roentgenology* 2004; **183**: 343–51. doi: <https://doi.org/10.2214/ajr.183.2.1830343>
18. Sibley CT, Huang J, Ugander M, Oki A, Han J, Nacif MS, et al. Myocardial and blood T1 quantification in normal volunteers at 3T. *J Cardiovasc Magn Reson* 2011; **13**(Suppl 1): P51. doi: <https://doi.org/10.1186/1532-429X-13-S1-P51>
19. Stanisz GJ, Odobina EE, Pun J, Escaravage M, Graham SJ, Bronskill MJ, et al. T1, T2 relaxation and magnetization transfer in tissue at 3T. *Magn Reson Med* 2005; **54**: 507–12. doi: <https://doi.org/10.1002/mrm.20605>
20. Morrow JM, Sinclair CDJ, Fischmann A, Reilly MM, Hanna MG, Yousry TA, et al. Reproducibility, and age, body-weight and gender dependency of candidate skeletal muscle MRI outcome measures in healthy volunteers. *Eur Radiol* 2014; **24**: 1610–20. doi: <https://doi.org/10.1007/s00330-014-3145-6>
21. Zhang X, Petersen ET, Ghariq E, De Vis JB, Webb AG, Teeuwisse WM, et al. In vivo blood T(1) measurements at 1.5 T, 3 T, and 7 T. *Magn Reson Med* 2013; **70**: 1082–6. doi: <https://doi.org/10.1002/mrm.24550>
22. Li K, Dortch RD, Welch EB, Bryant ND, Buck AKW, Towse TF, et al. Multi-parametric MRI characterization of healthy human thigh muscles at 3.0 T - relaxation, magnetization transfer, fat/water, and diffusion tensor imaging. *NMR Biomed* 2014; **27**: 1070–84. doi: <https://doi.org/10.1002/nbm.3159>
23. Scheel M, von Roth P, Winkler T, Arampatzis A, Prokscha T, Hamm B, et al. Fiber type characterization in skeletal muscle by diffusion tensor imaging. *NMR Biomed* 2013; **26**: 1220–4. doi: <https://doi.org/10.1002/nbm.2938>
24. Polgar J, Johnson MA, Weightman D, Appleton D. Data on fibre size in thirty-six human muscles. An autopsy study. *J Neurol Sci* 1973; **19**: 307–18. doi: [https://doi.org/10.1016/0022-510x\(73\)90094-4](https://doi.org/10.1016/0022-510x(73)90094-4)
25. Edgerton VR, Smith JL, Simpson DR. Muscle fibre type populations of human leg muscles. *Histochem J* 1975; **7**: 259–66. doi: <https://doi.org/10.1007/BF01003594>
26. Brooks RA, Di Chiro G. Magnetic resonance imaging of stationary blood: a review. *Med Phys* 1987; **14**: 903–13. doi: <https://doi.org/10.1118/1.595994>
27. Lu H, Clingman C, Golay X, van Zijl PCM. Determining the longitudinal relaxation time (T1) of blood at 3.0 Tesla. *Magn Reson Med* 2004; **52**: 679–82. doi: <https://doi.org/10.1002/mrm.20178>
28. Wu W-C, Jain V, Li C, Giannetta M, Hurt H, Wehrli FW, et al. In vivo venous blood T1 measurement using inversion recovery true-FISP in children and adults. *Magn Reson Med* 2010; **64**: 1140–7. doi: <https://doi.org/10.1002/mrm.22484>
29. Sourbron SP, Buckley DL. Tracer kinetic modelling in MRI: estimating perfusion and capillary permeability. *Phys Med Biol* 2012; **57**: R1–33. doi: <https://doi.org/10.1088/0031-9155/57/2/R1>
30. Vincensini D, Dedieu V, Renou JP, Otal P, Joffre F. Measurements of extracellular volume fraction and capillary permeability in tissues using dynamic spin-lattice relaxometry: studies in rabbit muscles. *Magn Reson Imaging* 2003; **21**: 85–93. doi: [https://doi.org/10.1016/S0730-725X\(02\)00638-0](https://doi.org/10.1016/S0730-725X(02)00638-0)
31. Kumar D, Karampinos DC, MacLeod TD, Lin W, Nardo L, Li X, Majumdar S, Souza RB, et al. Quadriceps intramuscular fat fraction rather than muscle size is associated with knee osteoarthritis. *Osteoarthritis Cartilage* 2014; **22**: 226–34. doi: <https://doi.org/10.1016/j.joca.2013.12.005>